

Variability in Velocity Profiles During Free-Air Whisking Behavior of Unrestrained Rats

R. Blythe Towal¹ and Mitra J. Z. Hartmann^{1,2}

¹Department of Biomedical Engineering and ²Department of Mechanical Engineering, Northwestern University, Evanston, Illinois

Submitted 28 November 2007; accepted in final form 21 April 2008

Towal RB, Hartmann MJ. Variability in velocity profiles during free-air whisking behavior of unrestrained rats. *J Neurophysiol* 100: 740–752, 2008. First published April 24, 2008; doi:10.1152/jn.01295.2007. During exploratory behaviors, the velocity of an organism's sensory surfaces can have a pronounced effect on the incoming flow of sensory information. In this study, we quantified variability in the velocity profiles of rat whisking during natural exploratory behavior that included head rotations. A wide continuum of profiles was observed, including monotonic, delayed, and reversing velocities during protractions and retractions. Three alternative hypotheses for the function of the variable velocity profiles were tested: 1) that they produce bilateral asymmetry specifically correlated with rotational head velocity, 2) that they serve to generate bilaterally asymmetric and/or asynchronous whisker movements independent of head velocity, and 3) that the different profiles—despite increasing variability in instantaneous velocity—reduce variability in the average whisking velocity. Our results favor the third hypothesis and do not support the first two. Specifically, the velocity variability within a whisk can be observed as a shift in the phase of the maximum velocity. We discuss the implications of these results for the control of whisker motion, horizontal object localization, and processing in the thalamus and cortex of the rat vibrissal system.

INTRODUCTION

When an animal or robot moves its sensory surfaces through the environment, the velocities of the sensors necessarily affect the sensory data acquired. If the world is static relative to the timescale of the movement, the only variations in the sensory data are generated by the movement itself. This means that the “flow” of incoming information can be modified by the animal merely by altering the velocities of its sensory surfaces.

The rat vibrissal system is widely used to study the relationship between an animal's movements and the sensory data it acquires (Carvell and Simons 1990; Kleinfeld et al. 1997; Welker 1964). We have recently demonstrated that during natural exploratory behaviors, the rat alters the symmetry of its whisking movements to accommodate for rotational head velocity (Towal and Hartmann 2006). Specifically, the positional asymmetry between the right and left arrays was found to equal the angular distance that the head will move over the duration of the whisk. We call this asymmetry the “look-ahead” distance because the whiskers are probing in advance the space where the rat's head will be at the time of the next whisk. Presumably, this behavior helps ensure that the rat's head does not collide with objects.

The present study was undertaken to quantify variability in the velocity profiles of whisking during natural exploratory

behavior that included head rotations. Initial analysis showed that although most retractions consisted of smooth, monotonic velocity profiles, the majority of protractions departed widely from these smooth trajectories. Most notably, a significant number of the protractions actually reversed direction during the course of the protraction. Three alternative hypotheses for the function of the variable velocity profiles were then tested: 1) that they produce bilateral asymmetry specifically correlated with rotational head velocity, 2) that they serve to generate bilaterally asymmetric and/or asynchronous whisker movements independent of head velocity, and 3) that the different profiles—despite increasing variability in instantaneous velocity—reduce variability in the average whisking velocity. Our results favor the third hypothesis and do not support the first two.

The variability present in whisking velocity profiles has many behavioral and neurophysiological consequences for the animal. We discuss the implications of the variable velocity profiles for motor control of whisking, horizontal position encoding, and thalamocortical processing in the whisker–barrel system.

METHODS

All procedures were approved in advance by Northwestern's Animal Care and Use Committee and previously described in detail (Towal and Hartmann 2006).

Behavioral training

Three adult female (4–7 mo old) Long–Evans rats were water restricted during 1 mo of training and videography. Rats were trained to poke their heads out of the cage tunnel and explore completely empty space for 8–20 s, after which time a water reward was delivered through a pipette positioned at a random angle at constant height (Fig. 1A). Infrared lighting (>880 nm) was used to illuminate the search space, ensuring that the rat had no visual cues about reward location (Birch and Jacobs 1975; Deegan and Jacobs 1993). Auditory and olfactory cues were minimized. We found no side biases either in the whisking patterns on either side of the search space or in the amount of time the rats spent searching either side of the search space.

High-speed videography

Rats were filmed from two orthogonal angles at 250 frames per second (fps) using two high-speed video cameras (FastCam PCIs, Photron, San Diego, CA). One camera captured a “bird's-eye view” of the search space. The second camera captured a side view of the rat to monitor head tilt out of the horizontal plane. Analysis was restricted

Address for reprint requests and other correspondence: M. Hartmann, Mechanical Engineering, Northwestern University, 2145 Sheridan Road, Evanston, IL 60208-3107 (E-mail: m-hartmann@northwestern.edu).

The costs of publication of this article were defrayed in part by the payment of page charges. The article must therefore be hereby marked “advertisement” in accordance with 18 U.S.C. Section 1734 solely to indicate this fact.

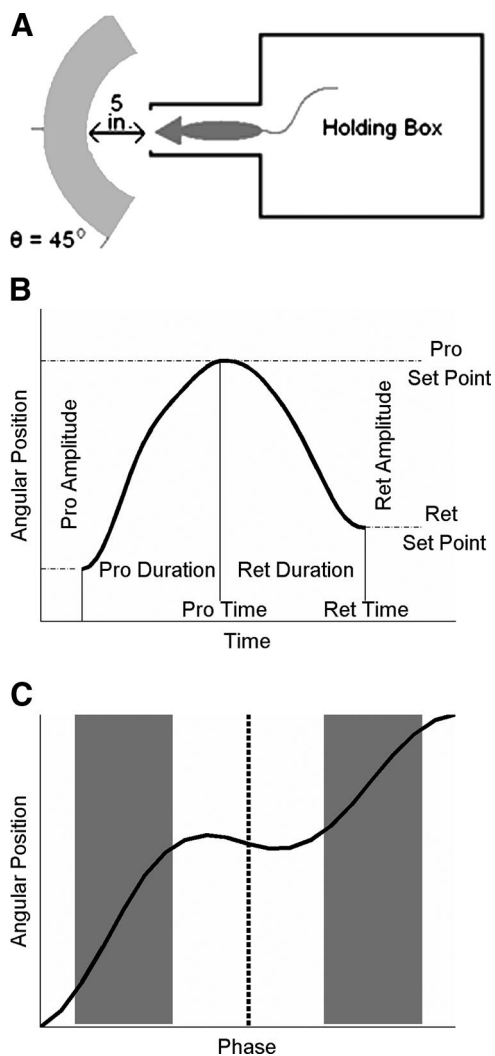


FIG. 1. Experimental setup and whisker parameters. *A*: top view of the behavioral setup. Shaded arc represents the possible reward locations, beginning 5 in. from the center of the tunnel and spanning 3 in. radially outward. *B*: schematic of a typical whisk, defining the morphological whisker parameters. *C*: an exemplary double-pump protraction illustrates the calculation of “start” and “end” velocities. Dashed line indicates the division of the whisk at the phase of the minimum velocity of the double pump. Gray bars show the regions of the whisk segment used to calculate the start and end velocities.

to those video clips in which the head and the macrovibrissae were visible and well focused. These clips corresponded to instances in which the head was sufficiently horizontal to lie within the depth of field of the top view camera.

Video analysis

As in previous work (Towal and Hartmann 2006), video data were imported into Matlab 7.0 (2005, The MathWorks, Natick, MA) as TIF files. The horizontal angular position of the head was found by manually locating the tip of the nose and the junction of the ears with the head. The head angle was then defined to be the angle of the line that connected the tip of the nose with the average of the two ear points. As reported previously, the average error in tracking the head angle was $0.06 \pm 0.56^\circ$, with a maximum error of 3.38° .

The angular positions of the two most-rostral and two most-caudal whiskers were manually tracked on both right and left sides along the initial (approximately linear) portion of the whisker. Average tracking error for the rostral whiskers was $6 \pm 4.5^\circ$, with a maximum error of

8° . Tracking error for the caudal whiskers was on average $1.5 \pm 4.5^\circ$ and had a maximum of 2° . The most-rostral whisker tracked was typically in the fourth column. Across all trials, the most-rostral whisker ever tracked belonged to the sixth column, ensuring that all whiskers tracked in this study were actuated by sling muscles (Dörfl 1982). Following the nomenclature of Wineski (1983), each whisk was then classified based on its velocity profile as a “single,” “delayed,” or “double” pump.

Coordinate systems for quantifying whisker trajectories

We analyzed whisker movements in a “snout-based” coordinate system in which the $0\text{--}180^\circ$ axis was defined along the caudal–rostral midline of the rat. This meant that protractions on both right and left sides were represented as increasing angular values and that symmetric whisking movements were represented as identical angles on the two sides of the face.

Four kinematic parameters were calculated for both the protraction and retraction segments of each whisk. These parameters are illustrated in Fig. 1*B* and include duration (the inverse of frequency), amplitude, average velocity, and set point. Supplemental Fig. S1¹ demonstrates that the distributions for these parameters are in agreement with previously published values (Berg and Kleinfeld 2003; Carvell and Simons 1990; Fee et al. 1997; Gao et al. 2001; Harvey et al. 2001; Hattox et al. 2003; Sachdev et al. 2003), including an average whisking frequency of 8.25 ± 2.24 Hz.

Note that peak protraction is defined as the time when protraction ended and retraction began. Similarly, peak retraction is defined as the time when retraction ended and protraction began. Thus both peak protraction and peak retraction have units of time. In contrast, the protraction set point is defined as the angle at which the protraction ended and retraction began and the retraction set point as the angle at which the retraction ended and protraction began. The set-point variables thus have units of degrees.

Normalizing whisker positions in terms of phase

In some analyses, whisker positions were normalized in time and reported in terms of phase. This allowed the comparison of whisker positions and velocities at the same phase of the whisk regardless of the variability in individual whisker parameters. Each normalized whisk was described by the whisker position at 20 uniformly distributed points in time for protraction and 20 uniformly distributed points in time for retraction. Thus each whisk was described by 40 phase points with peak protraction defined at 180° . The whisker position at each of these time points was found by linearly interpolating the tracked whisker positions. Protraction was defined to occur between 0 to 180 (π radians) degrees and retraction between 180 (π radians) and 360 (2π radians) degrees.

Effects of averaging across rostral and caudal whiskers

The data presented in RESULTS represent the average position of the rostral-most and caudal-most tracked whiskers (the “midarray” whisker angles). To eliminate the possibility that the delayed and double pumps were merely an artifact of the averaging process we classified the whisks of rostral and caudal whiskers separately. None of the conclusions of this study was significantly affected by using only the rostral or caudal whisker positions.

Effect of filtering the tracked data

Head and whisker angles were low-pass filtered to reduce tracking noise. Both vertical and horizontal head angles were filtered at 10 Hz.

¹ The online version of this article contains supplemental data.

Filtering the head angles at 20 Hz instead of at 10 Hz did not change any results of the present study.

All whisker angles were filtered at 25 Hz. Filtering the whisker angles at 20 or 30 Hz did not change any of the main conclusions of this study, as demonstrated in Supplemental Figs. S2 and S3. However, changing the cutoff frequency significantly affected the distribution of velocity profiles described in the first section of RESULTS. We therefore performed a rigorous quantification to establish that 25 Hz was indeed the appropriate low-pass cutoff frequency for the whisking signal.

First, we determined the frequency at which the whisking signal strength was significantly larger than the tracking error. To do this, we calculated the power spectrum of each trial from 1 to 125 Hz. The tracking error can then be observed in the power spectrum as the asymptote of the signal strength. The mean signal strength for frequencies from 100 to 125 Hz was calculated to be 0.378 units/Hz and a linear regression on these 25 frequency points indicated that the slope of the power spectrum in this region was not significantly different from zero (two-tailed *t*-test, $P = 0.67$). This value was therefore used as the asymptotic value. On average, across all trials and animals, the highest frequency that differed from the asymptotic value was 23 ± 2.5 Hz. We therefore chose 25 Hz as the most appropriate filtering frequency. Filtering above 25 Hz will contaminate the whisking signals with noise, whereas filtering at a lower frequency will neglect important signal features.

Although changing the filtering frequencies for the tracked whisker data substantially changed the fraction of whisks that were classified as single, delayed, or double, it is important to note that the main results of this study were completely unaffected by filtering frequency. Supplemental Table S1 shows the percentages of each pump type when the whisker angles are filtered at 20 and 30 Hz, confirming that regardless of how the data were filtered, protraction still exhibited many more delayed and double pumps than did retraction. None of the conclusions of the present study relies on the exact classification of pumps or on the precise velocities of the whisksers.

Definition of a whisk segment and dividing each whisk segment into two parts

We define a whisk segment as either a protraction or a retraction, as schematized in Fig. 1B. Some analyses required us to compare the velocity at the “start” and the “end” of each whisk segment. To do this, we divided each whisk segment into two parts, as shown in Fig. 1C. For single pumps, the whisk segment was divided at its midpoint, defined in terms of phase. For delayed pumps, the whisk segment was divided at the phase of the lowest velocity within the delay. For double pumps, the whisk segment was divided at the phase of the most negative velocity of the double pump. The average velocity at the “start” and “end” of the whisk segment was then calculated over the regions shown by the gray bars in Fig. 1C. The gray bars were established by setting a phase threshold at $\pm 14^\circ$ (0.24 radians) from the segment start, segment division, and segment end. All whisk segments had reached a stable velocity within the regions defined by this phase criterion. This phase criterion avoided the inclusion of velocity values very close to zero, which would tend to contaminate the estimate of start and end speeds.

Statistical methods

The 325 whisks considered in our analysis came from 89 whisking bouts. At least one previous study has shown that at least one whisking parameter—whisking frequency—is relatively constant within a bout but varies widely between bouts (Berg and Kleinfeld 2003). This means that individual whisks cannot be considered independent samples. Instead, the possible correlations between whisk parameters within a bout had to be accounted for in any statistical calculation. To account for within-bout correlations

between whisk parameters, we used a mixed-model analysis. This type of analysis is commonly used to test for differences between factors in two-factor experiments in which one factor is set by the experimenter (the fixed factor) and the other factor is considered random (the random factor). Using this type of model, the components of the variance associated with the random factor are taken into account when computing the test statistics for differences between the fixed-factor groups.

In our analysis, we aimed to determine differences between a given whisk parameter (e.g., amplitude or asymmetry) across different velocity profiles, given the existence of correlations within a bout. Thus the fixed factor in our analysis was the velocity profile (i.e., the three whisk types) and the random factor was the whisking bout. The analysis was run assuming a compound symmetry model for the repeated covariance within a trial. Pairwise comparisons between the means for a given parameter across different whisking profile types were assessed using the Bonferroni method within the context of the mixed-model analysis. The resulting *P* value and significance levels can be interpreted in the same way as an ANOVA, except that they do not require each whisk to be an independent sample. An α value of 0.01 is used throughout this study to test significance.

RESULTS

This study presents results from the analysis of 15,655 frames (62.62 s) of video data consisting of 89 bouts of whisking containing 325 distinct free-air whisks. These data were equally distributed between all three animals with just over 100 whisks for each rat. The whisks were taken from 43 bouts for rat 1, 25 bouts for rat 2, and 21 bouts for rat 3. The number of bouts is not equal across rats because the length of a typical whisking bout is highly variable (1–10 s; e.g., Berg and Kleinfeld 2003; Welker 1964). We first illustrate the continuum of velocity profiles present during natural behavior and then investigate three alternative hypotheses for the function of the variable velocity profiles.

Three exemplary velocity curves capture the continuum of velocity profiles

Figure 2 presents exemplary position and velocity profiles during protraction and retraction. The figure reveals a continuum of velocity profiles, which could be classified based on the sign of their velocity curve as “single pumps,” “delayed pumps,” or “double pumps.” This nomenclature was first suggested by Wineski (1983).

Figure 2 (*first three columns*) depicts examples of “Single Pumping,” defined as a protraction or retraction that monotonically increased or decreased with a roughly sigmoidal shape. This profile was mathematically identified by a positive or negative velocity maintained throughout the whisk segment. “Delayed Pumping” (Fig. 2, *middle three columns*) consisted of whisker movements that increased or decreased monotonically, but had complex shapes, indicating that the whisksers slowed down during their trajectory. These whisks were classified by a velocity that came to within $\pm 0.05^\circ/\text{ms}$ of zero at some point between the start and the end of the whisk segment. The $\pm 0.05^\circ/\text{ms}$ range was chosen because it represents roughly one tenth of the average whisk segment velocity. None of the conclusions of this study was affected by changing the cutoff range either to ± 0.1 or to $\pm 0.01^\circ/\text{ms}$. Further, changing the cutoff range did not alter the percentages of whisks classified as each type by more than 3% in any case.

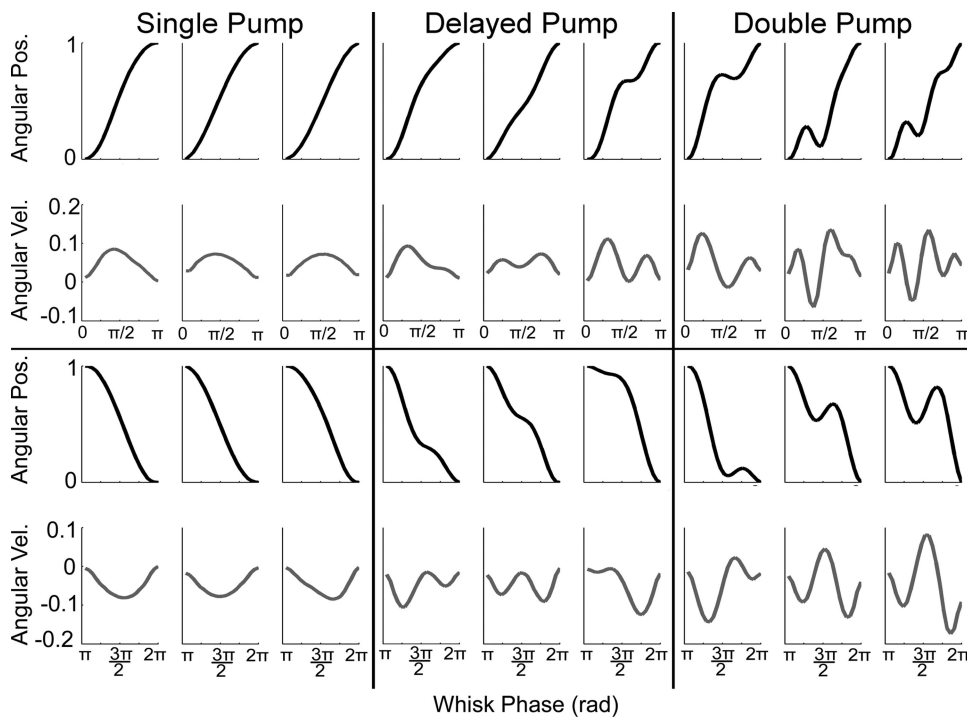


FIG. 2. Nine exemplary protraction and retraction segments illustrate the continuum of position and velocity profiles. Angular position has been normalized between zero and one. Angular velocity was calculated as the derivative of the normalized angular position. Both velocity and position are plotted as a function of phase. Thick black vertical lines indicate the separation of the continuum into the 3 profile types: single, delayed, and double.

Finally, Fig. 2 (last three columns) depicts “Double Pumping” protractions and retractions. Double pumping protractions have been described previously (Carvell and Simons 1990; Wineski 1983) and were defined as a movement in which the whisker partially retracted before reaching its most protracted angle. Similarly, double pumping retractions were defined as a movement in which the whisker partially protracted before reaching its most retracted angle. A whisk segment was classified as a double pump if the velocity changed sign during the whisk.

Table 1 lists the percentage of the 325 whisks that were classified as single, delayed, and double pumps. Although all three velocity profiles were observed during both protraction and retraction, they occurred in considerably different proportions. Most noticeably, retractions were dominated by single pumps (between 69 and 82%), whereas protractions were dominated by delayed and double pumps (between 76 and 79%). Differences in velocity profiles are also seen between rostral and caudal whiskers. Rostral whiskers exhibit fewer delayed but more double pumped

protractions than caudal whiskers. Rostral whiskers also exhibit fewer single retractions and more double and delayed retractions than caudal whiskers. Thus in general, the rostral whiskers performed more complex pumping patterns.

Pump types are not an artifact of vertical head motion

Because the camera used to measure whisker motion was fixed and the rat’s head could move relative to the image plane, it was possible that the presence of delayed and double pumps constituted an artifact of vertical head motion. For example, if the rat were to perform a single pump while rapidly tilting its head toward the ground, the whiskers could appear to delay or reverse in direction in our overhead camera. We ruled out this possibility in two ways. First, we determined that the velocity of head movements, both in the horizontal and vertical directions, is roughly ten times slower than the velocities of whisking movements. This means that, in general, any effect of head movements on the timescale of a single whisk segment is small.

TABLE 1. Frequency of profile occurrences for rostral, caudal, and “midarray” whiskers

Profile	Percentage of 325 Whisks Classified As:							
	Protraction				Retraction			
	Single	Delayed	Double	Delayed + Double	Single	Delayed	Double	Delayed + Double
Rostral	24%	29%	47%	76%	69%	11%	20%	31%
	23, 26, 13	29, 27, 25	48, 47, 62	77, 74, 87	66, 72, 88	12, 12, 0	22, 16, 12	34, 28, 12
Caudal	22%	43%	35%	78%	78%	8%	14%	22%
	24, 23, 0	43, 44, 50	33, 33, 50	76, 77, 100	77, 80, 75	7, 9, 12	16, 11, 13	23, 20, 25
“Midarray”	21%	44%	35%	79%	82%	7%	11%	18%
	20, 21, 6	42, 50, 61	38, 29, 33	80, 79, 94	79, 86, 83	9, 7, 6	12, 7, 11	21, 14, 17

Column 4 under both protraction and retraction is simply the sum of columns 2 and 3. Note that the percentage of “midarray” pumps is not the average of the rostral and caudal percentages. The classification of midarray profiles was based on the midarray angles, calculated as described in METHODS. The triple set of numbers below each percentage represent percentages of each whisk type separated by animal: rat 1, rat 2, and rat 3.

Second, we quantified the distribution of vertical head positions, vertical head speeds, and vertical head velocities during each type of pump. To eliminate the vertical head motion as an explanation for the different velocity profiles we performed two separate analyses on every head parameter (position, speed, velocity) separated by each pump type (single, delayed, double). First, a mixed-model analysis showed that the means of the vertical head positions, vertical head speeds, and vertical head velocities were not significantly different between the pump types [all $F_{(2, 299.5, 0.01)} < 4.7$, which means that $P > 0.01$ for all comparisons]. Second, a Bonferroni pairwise comparison of the means for each case showed no significant differences between any of the pump types, regardless of vertical head position, speed, or velocity ($\alpha = 0.01$). Vertical head motion can therefore be eliminated as the primary explanation for the observation of delayed and double pump whisk segments.

Bilateral coordination of pumping types

Left and right whisker arrays did not always perform the same type of whisk. For example, when the left array performed a single pump whisk, the right array did not necessarily also perform a single pump. A chi-squared analysis revealed that the left and right side pump types were not independent ($\chi^2 = 39.88$, $\text{dof} = 4$, $P > 0.01$). The residuals of the chi-squared analysis showed a positive association between the pump types, i.e., that single pumps on one side were more often associated with single pumps on the opposite side. To further quantify the nature of these bilateral relationships, we calculated the conditional probabilities for whisk types between the left and right whisker arrays.

First, we computed the probability that the right side would perform a particular type of whisk, given that the left side performed a particular type of whisk (the conditional probability). Figure 3 shows the values separated by protraction and retraction. When the left side performed a single pump protraction (Fig. 3, *top left*), the right side was roughly equally likely to perform each type of whisk, as indicated by the fact that all three bars are close to the 33% (chance) level. In contrast, when the left array performed a delayed or double pump during a protraction, the right array also performed a delayed or double pump roughly 50% of the time. Thus when a delayed or double pump protraction occurs on one side, a delayed or double pump is more likely on the opposite side. During retractions, however, the right side performed a single pump between 60 and 80% of the time, regardless of whether the left side performed a single, delayed, or double pump.

This analysis does not account for the fact that single, delayed, and double pumps already have different probabilities of occurrence, regardless of what type is occurring on the opposite side. Therefore in a second analysis, we calculated how the probability of a certain whisk type on each side was changed given that the opposite side performed a certain type of pump. In other words, we calculated the difference between the probability of a certain whisk type on the right side given a certain whisk type on the left side (conditional probability) and the probability that the whisk type would occur on the right side independent of the left side.

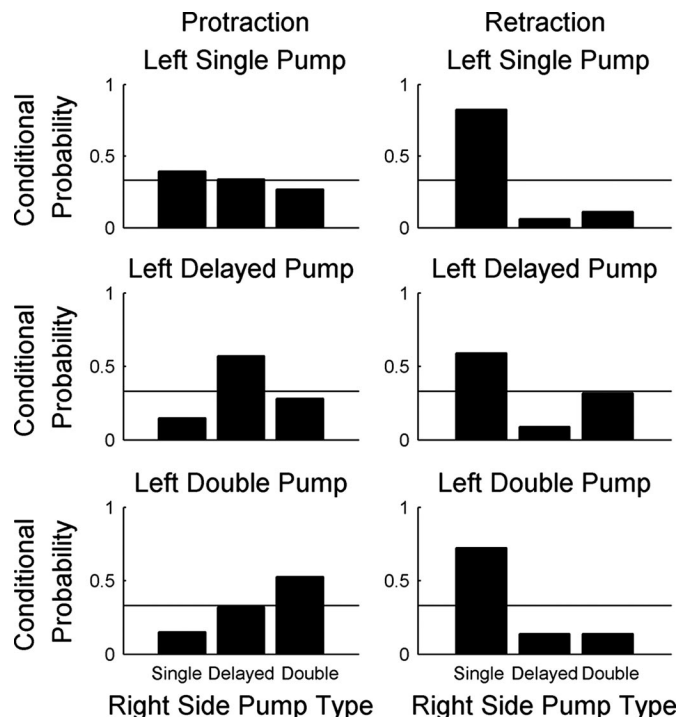


FIG. 3. Conditional probabilities of right side pump types given left side pump types. The height of each bar indicates the probability of observing a particular pump type on the right side (single, delayed, or double) given that a certain pump type occurred on the left side. Horizontal line indicates chance probability at 0.33.

Table 2 lists these values separated by protraction and retraction. The table shows that the maximum change in whisk type probability on the right side resulting from a particular whisk type occurring on the left side was -20.9% . This value indicates that when the left side performs a delayed pump retraction the right side is 20.9% less likely to perform a single pump retraction. Overall, the table shows that for protractions, the presence of a particular whisk type on the left side increased the probability of that same whisk type on the right side between approximately 13 and 20%. For retractions, the presence of a delayed pump on the left side increased the probability of a double pump on the right side by $\sim 18\%$ and decreased the probability of a single pump by $\sim 20\%$. The table also shows the change in probability separated by animal (comma separated numbers in each row). Although the probabilities are slightly different between animals, the same trends hold across all three rats. We can conclude from this analysis that, although the left and right side pump types are not completely independent of one another; the effect of the left side pump type on the right side pump type is typically small.

Kinematic parameters of single, double, and delayed whisks

We next investigated how different the kinematics of delayed and double pumps were from those of single pumps. The results presented in Fig. 4 illustrate that double and delayed pumps have average kinematic parameters quite similar to those of a single pump. First, Fig. 4, *A* and *B* shows that the average amplitudes of single and double pumps were not statistically different (mixed-model analysis, $P > 0.01$), for both protractions and retractions. Figure

TABLE 2. Change in probability of right whisk type given a particular left whisk type

Left Array Pump Type	Right Array Pump Type					
	Protraction			Retraction		
	Single Pump	Delayed Pump	Double Pump	Single Pump	Delayed Pump	Double Pump
Single pump	19.1%	-9.6%	-9.6%	2.5%	-0.9%	-0.2%
Delayed pump	20.2, 12.9, 5.6	-9.6, -21.1, -4.7	-11.6, -3.4, -8.9	-0.3, -0.3, -2.0	-2.1, 2.9, 0.3	1.8, -2.6, -0.7
Double pump	-5.5%	13.7%	-8.1%	-20.9%	0.2%	18.9%
	-2.5, -5.3, -5.6	10.3, 12.6, 8.2	-0.1, -7.9, -5.6	-12.7, -7.6, -8.2	-0.9, 1.3, 0	16.1, 22.7, 9.1
	-5.1%	-11.2%	16.4%	-7.6%	6.7%	0.9%
	-0.6, -13.9, -5.6	-0.5, -9.3, -6.7	10.1, 4.5, 11.1	-4.2, -17.4, -2.1	0.4, 2.2, 3.0	4.7, -5.2, 0.5

The percentages quantify the difference between observing a certain pump on the right side, $P(\text{right side pump})$, and observing a certain pump on the right side given that the left side has performed a given pump, $P(\text{right pump type} \mid \text{left pump type})$. For example, the upper left table cell may be read as: "The probability of observing a single pump on the right side is increased by 19.1% when the left side performs a single pump." Representing the probabilities in this way accounts for skewed distribution toward single pumps for retraction and double and delayed pumps for protractions. The triple set of numbers below each percentage represent percentages of each whisk type separated by animal: rat 1, rat 2, and rat 3.

4, *C* and *D* shows that the average set points were of similar magnitude during single, delayed, and double pumps (mixed-model analysis, $P > 0.01$). Finally, Fig. 4, *E* and *F* shows that the duration of the whisk segment increases by about 25% between single, delayed, and double pumps (mixed-model analysis, $P < 0.01$).

Investigating the behavioral function of double and delayed pumps

We next investigated three alternative hypotheses for the function of delayed and double pumps.

1) Delayed and double pumps serve to produce the specific type of bilateral whisking asymmetry correlated with rotational head velocity (Towal and Hartmann 2006).

2) Delayed and double pumps serve to generate bilaterally asymmetric and/or asynchronous whisker movements, independent of head velocity.

3) Delayed and double pumps allow for velocity variability within a whisk, while reducing variability in the average whisking velocity across whisks.

Evidence against Hypothesis 1: delayed and double pumps do not produce bilateral asymmetry correlated with rotational head velocity—in fact, they obscure the prediction of head motion

We have recently shown that the degree of bilateral whisker asymmetry is related to the angular distance that the head will move during the course of a whisk (Towal and Hartmann 2006). The results presented in Fig. 5 investigate whether the different velocity profiles might serve to maintain this anticipatory relationship. Figure 5*A* plots bilateral symmetry (left–right midarray whisker positions) versus head velocity, when single, delayed, and double pumped velocity profiles are grouped together. This figure is similar to Fig. 6*A* in Towal and Hartmann (2006) and illustrates the basic "looking-ahead" relationship, in which the difference in bilateral whisker positions is equal to the head velocity multiplied by the average duration of a whisk (110 ms).

Figure 5, *B–D* separates the data by velocity profile. The slopes and correlation coefficients of the data in Fig. 5, *A* and *B* are strikingly similar. In contrast, the relationships (slopes) shown in Fig. 5, *C* and *D* are significantly different from those in Fig. 5*B* (two-tailed t -test, $P < 0.01$), and the correlation coefficient for the data in Fig. 5*C* is significantly higher than that in Fig. 5*D* (two-tailed t -test, $P < 0.01$). These results suggest that as the complexity of the whisk segment profile increases to include at least one delayed or double pump, the "looking-ahead" relationship between whisker position and head velocity is increasingly obscured. Given that nearly all

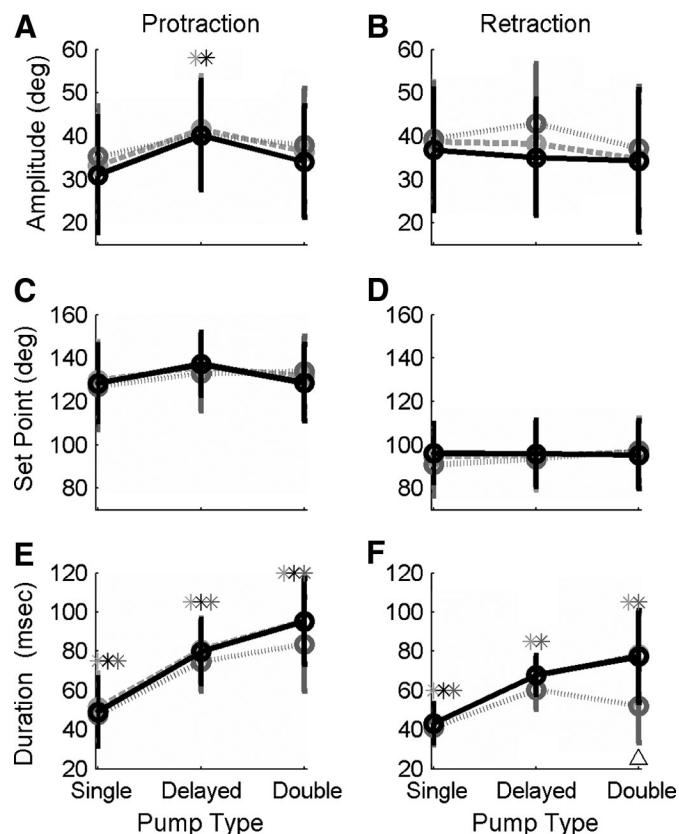


FIG. 4. Average whisk parameters for protractions and retractions. Distributions (mean and SD) of whisk amplitudes (*A*, *B*), set points (*C*, *D*), and durations (*E*, *F*), separated by rostral (dark gray, dotted), midarray (light gray, hashed), and caudal (black, solid) whiskers. Asterisks indicate that a parameter was statistically different for that pump type compared with the other 2 [mixed-model analysis (see METHODS), $P < 0.01$]. Asterisks are color coded to match the whisker colors described above. The Δ in the bottom right subplot indicates a significant difference between rostral whiskers and both midarray and caudal whiskers (mixed-model analysis, $P < 0.01$).

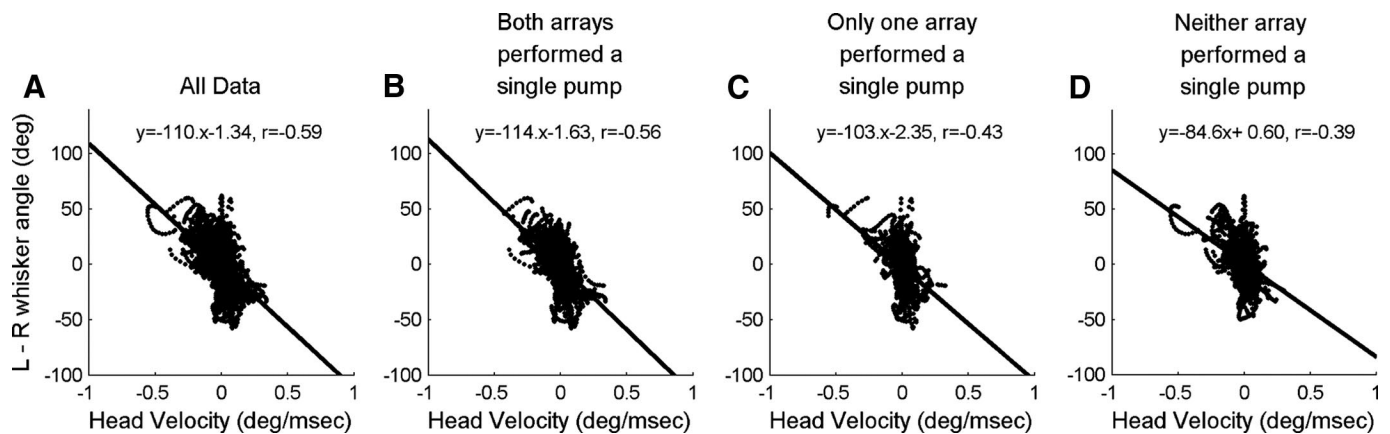


FIG. 5. A: the relationship (slope) between bilateral whisker asymmetry and the rotational head velocity when all whisking velocity profiles are grouped together ($n = 15,655$). B: when both arrays perform a single pump, the relationship (slope and correlation coefficient) between whisker asymmetry and head velocity remains similar to that in A ($n = 6,665$). C: when only one array performs a delayed or double pump, whisker asymmetry is less well correlated to head velocity than in A and B ($n = 3,714$). D: when both whisker arrays perform a delayed or double pump, the relationship between head velocity and whisker asymmetry is obscured even further ($n = 5,276$).

retractions consist of bilateral single pumps (Table 1), this result is consistent with the earlier finding that bilateral asymmetry is better correlated with rotational head velocity during the retraction segment of the whisk than during the protraction segment (Towal and Hartmann 2006).

Evidence against Hypothesis 2: delayed and double pumps do not serve to generate bilaterally asymmetric and/or asynchronous whisker movements

The previous section demonstrated that the different whisking velocity profiles do not serve to generate the asymmetric “looking-ahead” relationship observed during head rotations. However, it is still possible that double and delayed pumps provide the rat with a mechanism to induce particular asynchronies or asymmetries, independent of head velocity. If this were true, then particular asynchronies and/or asymmetries should be associated with the presence of a double or delayed whisk.

To test this hypothesis, we quantified the asymmetries and asynchronies both at the current whisk and at surrounding whisks. For a given sequence of whisks, the whisker asymmetry and asynchrony were calculated at: 1) the protraction and retraction set points of the current whisk, 2) the protraction and reaction set points of the preceding whisk, and 3) the protraction and retraction set points of the subsequent whisk. For each set of asymmetries and asynchronies, a mixed-model analysis was performed to determine whether the ranges of asymmetry and asynchrony were the same across bilateral pump types. The only evidence we found that the pump types were associated with bilateral asynchrony was found at the set point immediately after a particular velocity profile occurred [$F_{(8, 603.5, 0.01)} = 5.398, P = 0$]. Figure 6A illustrates this result. In general, the figure demonstrates that different velocity profiles are not correlated with bilateral asynchrony, with one small exception: namely, when the left side performs a double pump and the right side a single pump. Figure 6B quantifies the asymmetries at the set points immediately after a particular velocity profile has occurred, illustrating that whisker asymmetry is not related to any bilateral pump type combination.

Figure 6, A and B group the data over both protraction and retraction. When protraction and retraction were considered

separately, three bilateral protraction pump types generated statistically different asynchronies (Bonferroni pairwise comparison, $P < 0.01$): 1) when the left side performs a double pump and the right side a single pump, 2) when the right side performs a double pump and left side a single pump, and 3) when the left side performs a delayed pump and the right side a single pump. The reciprocal pairing of right side delayed pump with a left side single pump did not reach significance.

In summary, although there is some evidence for a correlation between pump type and asynchrony during protraction, the correlation is small and it seems unlikely that the function of the delayed or double pumps is to induce bilateral asymmetry or asynchrony.

Evidence in favor of Hypothesis 3

DIFFERENT VELOCITY PROFILES ALLOW VARIABILITY IN INSTANTANEOUS VELOCITY, AS EVIDENCED BY PHASE SHIFTS IN MAXIMUM VELOCITY. As shown earlier, the different velocity profiles do not primarily serve to generate the “look-ahead” distance or to generate bilateral asymmetry or asynchrony. In search of an explanation as to why the rat might choose to perform single, double, and delayed pumps, we quantified the detailed internal structure of the velocity profiles. We first investigated the relationship between whisking phase and the instantaneous whisking velocity.

The plots in Fig. 7 demonstrate that maximum velocity is reached at different phases of the whisk for each type of velocity profile. Figure 7A shows the average velocity profile of the middle whisks, for single, delayed, and double pumps plotted in polar coordinates. The angle indicates the phase of the whisk. The radial distance at each angle on the plot indicates the velocity at that phase of the whisk. Figure 7, B–D shows the average whisking profile for each type of whisk, as well as the variability of the profile indicated by 95% confidence limits (thin lines). Figure 7, E and F shows the same plots as those in Fig. 7A, but for the velocities of the rostral (Fig. 7E) and caudal (Fig. 7F) whisks. Although the instantaneous velocities are slightly different for the rostral, midarray, and caudal whisks, the basic structure of the profiles is the same.

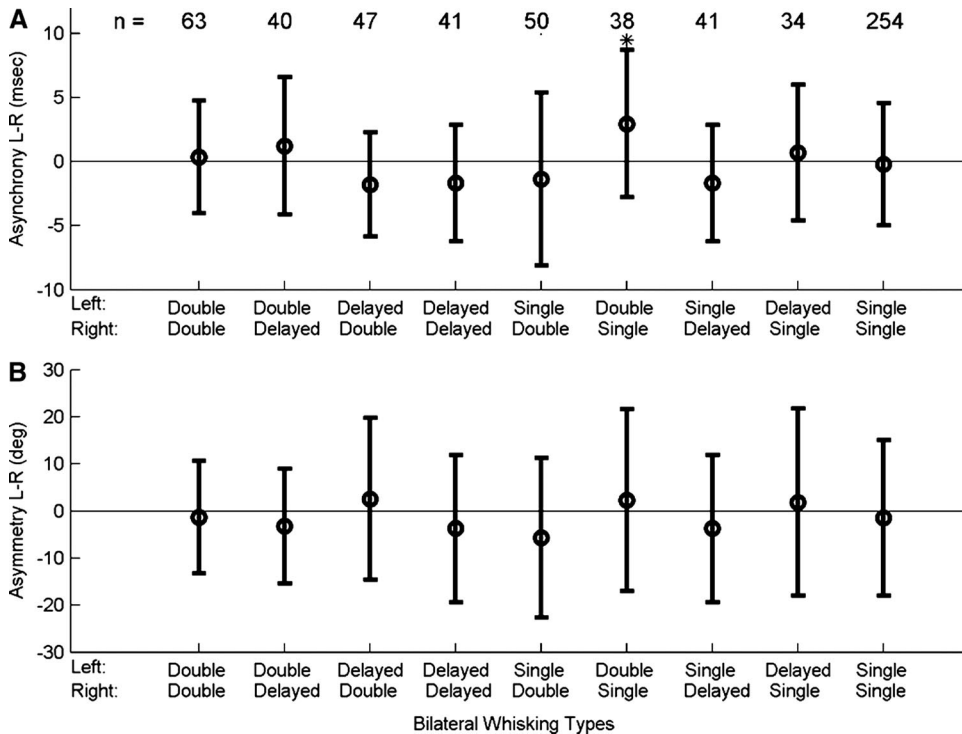


FIG. 6. Neither asynchrony nor asymmetry is associated with particular bilateral combinations of velocity profiles. *A*: for each of the nine bilateral combinations of whisk profiles, the left–right time difference of peak protraction and retraction was calculated. Means and SDs of the distributions are shown. Asterisk indicates the single distribution that was significantly different from zero (mixed-model analysis with Bonferroni pairwise comparisons, $P < 0.01$). The *x*-axis is roughly organized from complex whisks (Left Double, Right Double) to simpler whisks (Left Single, Right Single). The numbers listed at the top show the number of whisk segments in each category. The Single–Single category has a larger number of whisk segments because the majority of retractions are single pumped. *B*: the same plot as in *A*, showing the degree of asymmetry (left–right position difference) instead of the degree of asynchrony.

As expected, all three profiles approach zero velocity at 0 and 180° because they must change their direction at the start and end of protraction and retraction. However, it is clear that the profiles achieve their maximum velocities at different phases of the whisk. For example, the single pumps achieve maximum velocity at roughly 90 and 270°, in the middle of the protraction and retraction. In contrast, the delayed and double

pumps achieve a high velocity twice during each whisk segment, near 40, 150, 220, and 320°.

VELOCITY PROFILES PERMIT VELOCITY VARIABILITY WITHIN A WHISK WHILE REDUCING VARIABILITY IN THE AVERAGE WHISKING VELOCITY ACROSS WHISKS. The results of Fig. 7 demonstrate that the different pump types are accompanied by an increase in vari-

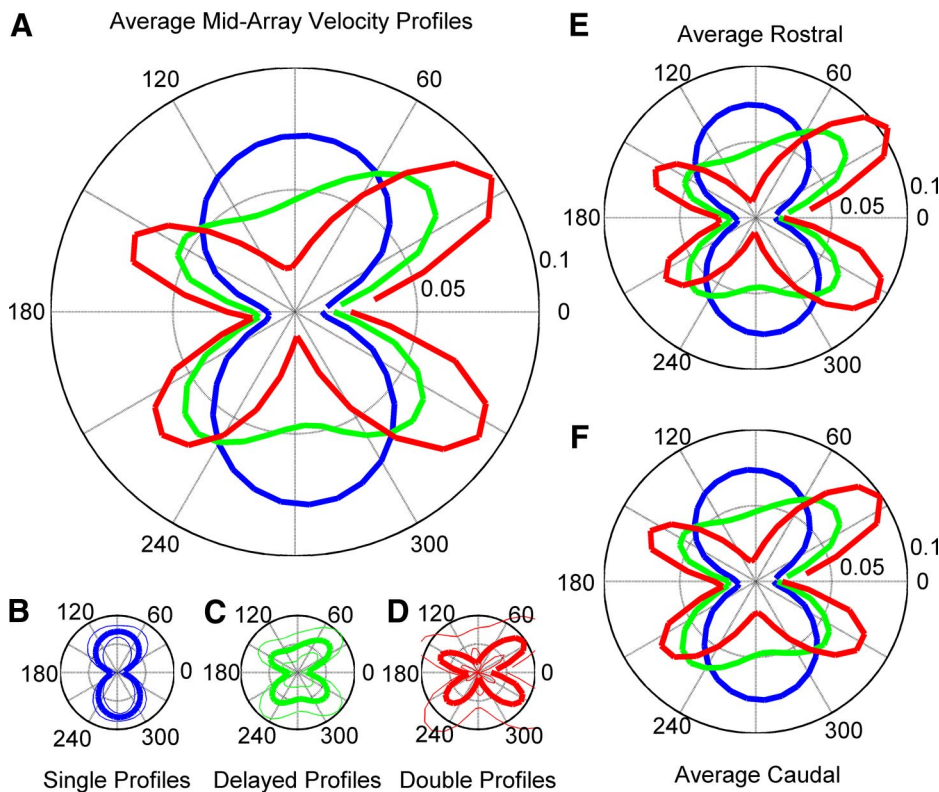


FIG. 7. Phase of maximum velocity varies across velocity profiles. *A*: polar plot of averaged, normalized velocity profiles for the midarray whisker angles. Radial distance represents whisk velocity (deg/ms) calculated from the normalized whisker position. The radial axis has the same range for all plots. Angle represents whisk phase, with protraction defined from 0 to 180° and retraction from 180 to 360°. Blue, single pumps; green, delayed pumps; red, double pumps. *B–D*: average profile as in *A* (thick line), with 95% confidence limits imposed (thin lines) for single (*B*), delayed (*C*), and double pumps (*D*). *E*: the same plots as in *A*, but for the rostral whiskers. The maximum value of the double pumps (red) is 0.104 deg/ms. *F*: the same plots as in *A*, but for the caudal whiskers.

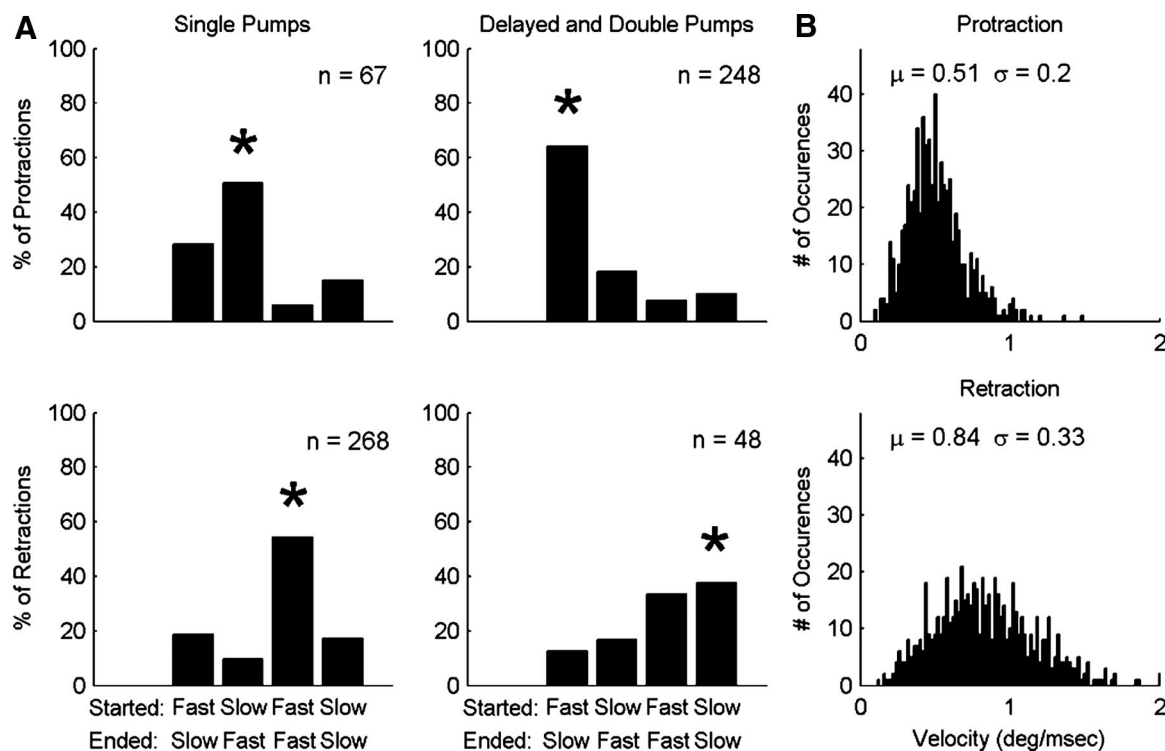


FIG. 8. Velocity compensation during whisk segments. *A*: the ordinate of each subplot groups whisks into four categories based on the start and end whisk velocities. *Top row*: percentage of protractions that fell into each category, for different velocity profiles. *Bottom row*: percentage of retractions in each category. Asterisks indicate the largest category in each subplot, all of which were statistically different from the other categories (χ^2 test, $P < 0.001$). *B*: the distribution of average velocities separated by protractions (*top row*) and retractions (*bottom row*). μ - mean, σ - standard deviation.

ability of the instantaneous whisking velocity. We next investigated the possibility that despite the increased variability in the instantaneous velocity, the different whisking profiles actually reduce whisking velocity variability on average. In other words, the different pump types could correct for an initial “error” in the velocity of the whisk segment. For example, if a whisk segment started “too fast,” a delayed or double pump could slow down the whisk segment velocity midcycle.

To perform this analysis, each whisk segment was divided into two parts and the velocity of each part was calculated (see Fig. 1C in METHODS). A protraction (retraction) was defined as “starting slow” if the velocity of the first part was less than the average of all 325 protraction (retraction) velocities. A protraction (retraction) was defined as “starting fast” if the velocity of the first part was greater than the average of all 325 protraction (retraction) velocities. Each whisk segment was then separated into one of four categories.

1) Start fast, end slower: The whisk segment started fast and ended slower than it started.

2) Start slow, end faster: The whisk segment started slow and ended faster than it started.

3) Start fast, end faster: The whisk segment started fast and ended either at the same speed or faster than it started.

4) Start slow, end slower: The whisk segment started slow and ended either at the same speed or slower than it started.

Figure 8A shows the percentage of whisk segments (protractions and retractions) that fall into each of the four categories. The two leftmost bars in each subplot (Fast/Slower and Slow/Faster) indicate a compensatory change in whisk segment velocity. The two rightmost bars in each subplot indicate that velocity compensation did not occur over the course of the

whisk segment. Inspection of Fig. 8A reveals three key elements of natural free-air whisking kinematics. 1) The *top left plot* illustrates that during single pump protractions, the majority of whisk segments tend to compensate for the initial velocity. Approximately 79% of protractions fall into one of the two compensatory categories (Fast/Slower or Slow/Faster). More specifically, the majority (53%) of single pump protractions tended to start slow and end faster. 2) The *top right plot* illustrates that delayed and double pump protractions also tend to compensate for the initial whisk segment velocity. Approximately 82% of protractions fall into one of the two compensatory categories (Fast/Slower or Slow/Faster). However, in contrast to single pump protractions, the majority (64%) of delayed and double pump protractions tended to start fast and end slower. 3) The *bottom row* indicates that regardless of pump type, retractions tended not to compensate for initial whisk segment velocity, but rather to accentuate it.

Taken together, these results suggest that the average velocity over the whole protraction should tend to be more stable than the average velocity of the retraction. This expectation is supported by the data in Fig. 8B. The histograms in this figure illustrate that the whisk velocity averaged over a protraction tends to be less variable than the average retraction velocity. An *F*-test on the variance shows that the variance of protraction velocities ($\sigma_{\text{pro}}^2 = 0.04$, $n = 650$) is significantly smaller [$P < 0.01$, $F_{(6.81, 640, 0.01)} = 0.505$] than the variance of retraction velocities ($\sigma_{\text{ret}}^2 = 0.11$, $n = 650$). Note that although Fig. 8, A and B shows data for the middle whisker angles only, the same results were found for both rostral and caudal whisks.

Thus far, we have shown that different velocity profiles permit maximum velocity to be achieved at different phases of

the whisk (Fig. 7), while maintaining a relatively consistent average velocity over the course of a whisk segment (Fig. 8). One caveat to this result, however, is that the phase of maximum velocity might not be behaviorally relevant to the rat. We need to consider an alternative interpretation of the data presented in these figures.

The alternative interpretation is easiest to explain in the form of an example that anthropomorphizes the rat: Suppose that the rat wants to “select” some particular velocity at some particular phase within the whisk. The particular velocity the rat wants could take on any value, and the particular phase at which the rat wants that velocity to occur could also take on any value. In this experiment, we are not able to judge what velocity or phase the rat may be interested in. When we plot the data as in Fig. 7, we merely observe the rat’s selection of a particular combination of parameters as a phase shift in the maximum velocity.

DISCUSSION

The present study quantifies the velocity profiles of free-air whisking protractions and retractions in awake rats during search behaviors that include head rotations. The profiles exhibit a high degree of variability, including both partial and complete direction reversals during protractions. These findings have substantial implications for the control of the whisking central pattern generator (CPG), horizontal position encoding, and thalamocortical processing in the whisker–barrel system.

Mechanical basis for different velocity profiles

The variability in velocity profiles that characterizes protractions (and, to a lesser degree, retractions) suggests a corresponding variability in muscle activation. Several studies have shown that whisking protractions are dominated by the activation of the intrinsic muscles, whereas retraction is primarily under the control of the extrinsic muscles (Berg and Kleinfeld 2003; Dörfel 1982; Hill et al. 2006). In our video analysis, whisker angles were measured near the base of the whisker as it emerged from the mystacial pad. This means that, by definition, during a single pump protraction, the whiskers are continuously increasing in angular position, suggesting that intrinsic muscles are dominating the movement. In contrast, during a delayed or double pump protraction, the whiskers are not always moving rostrally—sometimes they are moving caudally. At these times the intrinsic muscles are likely to be decreasing their activation relative to the extrinsic muscles. Although our results cannot determine which muscles are responsible for the delayed and double pump whisking profiles, they do strongly suggest that the rat is likely to have precise control over the protraction. In particular, the presence of double pumps suggests that the rat may be able to reset the whisk in the middle of protraction.

Implications of delayed and double pumps for the whisking CPG

An intriguing possibility for the function of delayed and double pumps is that they are used to selectively sample a particular region of the environment at different times, phases, or positions within the whisk. This would mean that the

complex velocity profiles associated with protraction are under more cognitive control, as the rat seeks out regions of the space particularly salient to the current behavioral task. Velocity profiles during retraction are consistently more stereotyped than those during protraction (Table 1). As suggested previously (Carvell and Simons 1990; Welker 1964) this increased stereotypy may indicate that the retraction segment is less under cognitive or voluntary control and more constrained by biomechanics.

An analogy might be made to the central pattern generator (CPG) associated with rat licking behavior, which occurs at a regular frequency of about 6 Hz (Brozek et al. 1996). When the licking CPG is electrically stimulated during tongue protrusion, the phase of the licking cycle can be reliably reset. In contrast, if the electrical stimulus is applied during tongue retraction, the licking cycle does not change. Although further investigation is needed to determine the extent to which pattern generation can be modulated during whisking, our data support a similar dichotomy for the putative whisking CPG: retraction is a mechanically constrained, more passive whisking segment over which the animal has little or no cognitive control.

Could double pumps actually be two separate whisks?

Periodic movements of the vibrissae were first described by Welker (1964) and were found to be synchronized with the sniffing cycle. Figure 2 of that study suggests that whisker movements during the sniffing cycle can be schematized as smooth, single-pump protractions and retractions. This schematic view of the whisk has tended to dominate the subsequent literature: a single whisk is typically thought to consist of a rostral-sweeping protraction and a caudal-sweeping retraction. This means that a smooth velocity profile tends to be implicitly embedded within the literature’s definition of a “whisk.”

Along with the work of Wineski (1983), who coined the phrase “double-pump,” the present results suggest that quantification of natural whisking behaviors requires a definition of a “whisk” that does not depend on a monotonic velocity profile. Recent results from the Kleinfeld laboratory have been gradually enabling a more mechanistic definition of the whisk, based on patterns of muscle activation (Berg and Kleinfeld 2003; Hill et al. 2006). In this context, it is important to consider the possibility that double pumps are in fact two separate whisks with very different set points. Whether a double pump consists of a single, complex “whisk,” or consists of two simpler single-pump “whisks” has important implications for control of the putative whisking CPG.

Consider two cases: (A) The double pump is a single, albeit complicated, whisk. (B) The double pump is actually two whisks in rapid succession, with the midphase velocity reversal constituting a brief retraction. In case A, each whisk will have similar set points and durations (see Fig. 4), but will have a highly variable velocity profile. This is the description we have chosen to use throughout the present manuscript. In case B, however, each whisk is made up of single pumps with highly variable set points and durations, and smaller than average amplitudes.

In case A, delayed and double pump velocity profiles could be caused by delays between the activation of different muscle groups. This would mean, in turn, that elements of the CPG circuitry would need to modulate the delay

between activation of the different groups. In contrast, case B would require elements of the CPG to vary the start time (or frequency) and position (or set point) of each whisk cycle, whereas the delays between muscle group activations could remain constant.

As suggested in RESULTS, we favor the interpretation consistent with case A—that double pumps represent a “single whisk.” Our view is based on the observation that double, delayed, and single pumps all contain roughly the same kinematic structure. First, as shown in Fig. 4, the set point and amplitudes of all pump types are similar. Second, the durations of double pumps are at most 25% longer than single pumps, not twice as long as would be expected if a double pump consisted of two single pumps. Future studies will require electromyography to more completely examine the patterns of muscle activation associated with each type of velocity profile.

Role of velocity in radial distance encoding

The present experiments involved whisking in free air, without any object contact. The animal's experience with the environment was that an object (the reward pipette) was equally likely to appear within any region of the search space. The whisking velocity profiles in this experiment thus capture the natural movements that an animal will make during the detection and localization portions of search behavior. These same velocity profiles cannot be assumed to hold during object discrimination because contact with an object will almost certainly change them substantially (Carvell and Simons 1990a; Mitchinson et al. 2007; Wineski 1983).

During search behavior that involves detection and localization, the animal is unlikely to be concerned with detailed object properties such as texture. Instead, the animal is more likely to be concerned with determining the location of the object relative to its snout. Our laboratory has recently demonstrated that one plausible method for the rat to determine the radial distance to an object is to monitor the ratio of rate of moment change at the whisker base to angular velocity (*Eq. 7* in Birdwell et al. 2007). In that same paper, we also suggested that there may be particular combinations of these variables that would lead to improved sensitivities to particular radial distances. This computation would work even if the rat monitored instantaneous rates of change only in these variables. This means that the computation could be performed at every instant in time, as would be required during the initial detection portion of search behavior.

In the present study, we have provided evidence that the rat can generate substantial variations in whisking velocity during protraction, lending indirect behavioral support to this mechanical encoding mechanism. In particular, it may be useful for the rat to be able to choose particular velocities at particular temporal and/or spatial locations within the whisk, to scale the relationship between rate of change of moment and radial distance. In general, higher velocities will provide better resolution for objects further away (see Fig. 6A in Birdwell et al. 2007).

Velocity profiles support a horizontal localization scheme based on direct encoding of position information

A recent study has shown that rats can use a single whisker to localize an object along the rostrocaudal (horizontal) axis

(Mehta et al. 2007). However, the neural encoding mechanism that underlies horizontal localization is as yet unclear. There are currently two prominent hypotheses for the computation of horizontal location. One hypothesis predicts that the nervous system performs coincidence detection between the responses of contact-sensitive and position-sensitive neurons (Mehta et al. 2007; Szwed et al. 2003) to determine the horizontal angle of an object. This hypothesis requires that neurons encode whisker contact time as well as whisker position. A second hypothesis predicts that the time of whisker contact is computed as a function of whisking phase to determine the horizontal angle of an object (Ahissar 1998; Ahissar and Arieli 2001; Szwed et al. 2003). This theory requires the encoding of whisker velocity and the temporal delay between whisk onset and whisker/object contact.

Notably, many studies have shown that the responses of trigeminal ganglion neurons contain information about the time of whisker contact (Leiser and Moxon 2006; Szwed et al. 2003, 2006), whisker position or amplitude (Arabzadeh et al. 2005; Gibson and Welker 1983a,b; Jones et al. 2004; Leiser and Moxon 2006; Shoykhet et al. 2000; Szwed et al. 2003; Zucker and Welker 1969), whisk onset (Leiser and Moxon 2006; Szwed et al. 2003), and whisker velocity (Arabzadeh et al. 2005; Gibson and Welker 1983a,b; Jones et al. 2004; Leiser and Moxon 2006; Shoykhet et al. 2000; Zucker and Welker 1969). All of these parameters (except whisk onset) have been observed during passive stimulation of the anesthetized rat, during artificial whisking in the anesthetized rat, and during behaviors of the awake, freely moving rat. Thus all of the kinematic information needed for either hypothesis is available to the whisker system.

The present data argue against the second hypothesis for horizontal object localization in two respects. First, the relationship between whisk phase and external space is unique only when the whisker position monotonically increases through the whisk—in other words, when the whisker performs a single or delayed pump. However, when a reversal in direction occurs, the relationship between whisk phase and external space becomes non-unique: the same spatial location is achieved at three distinct phases of the whisk. Thus, potential neural computations used to determine position in the rostrocaudal plane from the phase of contact would seem to break down for any whisk that contained a velocity reversal.

Second, our data imply that the velocity must be taken into account at every instant to obtain an accurate representation of the whisker's position. The second hypothesis relies on a constant velocity to make use of the relationship: distance equals velocity multiplied by time (Ahissar 1998; Ahissar and Arieli 2001; Ahissar et al. 2000). Results from at least two laboratories have now shown that whisking velocity is highly variable between the two sides of the rat's face, both between whisks (Mitchinson et al. 2007; Towal and Hartmann 2006) and within a whisk (present study). Thus the position of the whiskers cannot be predicted by assuming that the whisker position equals whisking velocity multiplied by the time since whisk onset, as required by the second hypothesis. Instead, our data favor the first hypothesis. By directly measuring whisker position, the delayed and double pumps no longer pose a problem for calculating the spatial position of contact.

Implications of delayed and double pumps on thalamocortical processing of whisker input

Previous studies have shown that rat barrel cortex responds preferentially to high-velocity inputs. Specifically, high-velocity, passive whisker movements produce highly synchronized responses in the ventral posterior medial thalamus (VPm), which in turn produce strong responses in the layer 4 barrel cortex (Pinto et al. 1996, 2000; Temereanca and Simons 2003). Notably, large amplitude passively applied movements did not evoke strong responses in the cortex despite causing high thalamic firing rates (Pinto et al. 2000); instead, the strength of cortical responses (in number of spikes and duration of response) was found to be directly proportional to whisker velocity.

Our results have shown that different whisking velocity profiles achieve maximum velocity at different phases of the whisk. By shifting the phase of maximum velocity, the rat could, in effect, be shifting the phase of the whisk when the largest activity is induced in the cortex. Although it is unclear what the behavioral or computational motivation for this shift might be, the variable profiles suggest that the rat does have active control over the phase of the whisk at which the maximum whisker velocity is achieved. A related possibility is that double and delayed pumps may shift the protraction segment of the whisk relative to intrinsic thalamocortical oscillations. Delayed and double pumps may serve as a mechanism to shift the velocity or external position of the whiskers relative to the intrinsic dynamics of thalamocortical processing. These shifts could modify or gate the information transmitted to the cortex.

General importance of velocity during active sensing behaviors

As a sensor array moves through the environment, changes in the incoming data can be generated by movements of the environment as well as the sensor itself. The relationships between spatial and temporal aspects of the incoming sensory data can be expressed using the complete derivative (Gopal and Hartmann 2007). During rat whisking behavior specifically, we can relate how the radial distance from the base of a whisker to an object will change over time, to the spatial gradients of radial distance that exist across the whisker array at a single point in time

$$\frac{dR}{dt} = \frac{\partial R}{\partial t} + \bar{v}_{rel} \cdot \nabla R \quad (1)$$

In this equation, R represents the radial distance from the base point of any given whisker to the object, t is time, v_{rel} is the relative velocity between the whisker and the object, and ∇ is the gradient operator. If the environment is static relative to the timescale of the velocity of the whisk, then $\partial R/\partial t$ becomes zero and v_{rel} simply becomes the whisk velocity, allowing the animal to predict in advance how R should change with respect to time. To obtain the best prediction, however, the sensor needs to move at a velocity relevant to the spatial structure of the environment. The data presented here suggest that the rat may be able to change the whisking velocity in real time to modify the flow of incoming sensory information, directly enabling this type of prediction.

ACKNOWLEDGMENTS

We thank B. Paul and A. Ullom, along with M. Boen, J. Crystal, N. Naik, B. Quist, A. Kaloti, and A. Birdwell, for help with the behavioral training and for helping to track vibrissal locations; D. Pinto, P. Knutsen, D. Kleinfeld, and E. Ahissar for useful discussions; and A. Rademaker and I. Helenowski for help with the statistical methods used here.

GRANTS

This work was supported by an award from the Bio-Inspired Technologies and Systems/Center for Integrated Space Microsystems at the Jet Propulsion Laboratory, National Aeronautics and Space Administration; National Science Foundation Grants IOB-0446391 and IIS-0613568; and an award to the team of Northwestern undergraduate students from the Office of Industry Relations of the McCormick School of Engineering and Applied Science on behalf of The Ford Motor Company.

REFERENCES

- Ahissar E. Temporal-code to rate-code conversion by neuronal phase-locked loops. *Neural Comput* 10: 597–650, 1998.
- Ahissar E, Arieli A. Figuring space by time. *Neuron* 32: 185–201, 2001.
- Ahissar E, Sosnik R, Haidarliu S. Transformation from temporal to rate coding in a somatosensory thalamocortical pathway. *Nature* 406: 302–306, 2000.
- Arabzadeh E, Zorzin E, Diamond ME. Neuronal encoding of texture in the whisker sensory pathway. *PLoS Biol* 3: 155–165, 2005.
- Berg RW, Kleinfeld D. Rhythmic whisking by rat: retraction as well as protraction of the vibrissae is under active muscular control. *J Neurophysiol* 89: 104–117, 2003.
- Birch D, Jacobs G. Behavioral measurements of rat spectral sensitivity. *Vision Res* 15: 687–691, 1975.
- Birdwell JA, Solomon JH, Thajchayapong M, Taylor MA, Cheely M, Towal RB, Conradt J, Hartmann MJZ. Biomechanical models for radial distance detection by the rat vibrissal system. *J Neurophysiol* 98: 2439–2455, 2007.
- Brozek G, Zhuravin I, Megirian D, Bures J. Localization of the central rhythm generator involved in spontaneous consummatory licking in rats: functional ablation and electrical brain stimulation studies. *Proc Natl Acad Sci USA* 93: 3325–3329, 1996.
- Carvell G, Simons D. Biometric analyses of vibrissal tactile discrimination in the rat. *J Neurosci* 10: 2638–2648, 1990.
- Deegan JF, Jacobs GH. On the identity of cone types of the rat retina. *Exp Eye Res* 56: 375–377, 1993.
- Dörfl J. The musculature of the mystacial vibrissae of the white mouse. *J Anat* 135: 147–154, 1982.
- Fee MS, Mitra PP, Kleinfeld D. Central versus peripheral determinants of patterned spike activity in rat vibrissa cortex during whisking. *J Neurophysiol* 78: 1144–1149, 1997.
- Gao PH, Bermejo R, Zeigler HP. Whisker deafferentation and rodent whisking patterns: behavioral evidence for a central pattern generator. *J Neurosci* 21: 5374–5380, 2001.
- Gibson JM, Welker WI. Quantitative studies of stimulus coding in first-order vibrissa afferents of rats. 1. Receptive field properties and threshold distributions. *Somatosens Res* 1: 51–67, 1983a.
- Gibson JM, Welker WI. Quantitative studies of stimulus coding in first-order vibrissa afferents of rats. 2. Adaptation and coding of stimulus parameters. *Somatosens Res* 1: 95–117, 1983b.
- Gopal V, Hartmann MJZ. Using hardware models to quantify sensory data acquisition across the rat vibrissal array. *J Bioinspir Biomimet* 2: S135–S145, 2007.
- Harvey MA, Bermejo R, Zeigler HP. Discriminative whisking in the head-fixed rat: optoelectronic monitoring during tactile detection and discrimination tasks. *Somatosens Mot Res* 18: 211–222, 2001.
- Hattox AM, Li Y, Keller A. Serotonin regulates rhythmic whisking. *Neuron* 39: 343–352, 2003.
- Hill D, Bermejo R, Zeigler HP, Kleinfeld D. Biomechanics of the vibrissa motor plant in rat: rhythmic whisking consists of triphasic neuromuscular activity. *J Neurosci* 28: 3438–3455, 2008.
- Jones LM, Lee S, Trageser JC, Simons DJ, Keller A. Precise temporal responses in whisker trigeminal neurons. *J Neurophysiol* 92: 665–668, 2004.
- Kleinfeld D, Mitra PP, Fee MS. Motor modulation of sensory input: exploratory whisking by rat as a model system. *Somatosens Mot Res* 14: 63–63, 1997.
- Leiser SC, Moxon KA. Responses of trigeminal ganglion neurons during natural whisking behaviors in the awake rat. *Neuron* 53: 117–133, 2006.

- Mehta SB, Whitmer D, Figueroa R, Williams BA, Kleinfeld D.** Active spatial perception in the vibrissa scanning sensorimotor system. *PLoS Biol* 5: 309–322, 2007.
- Mitchinson B, Martin CJ, Grant RA, Prescott TJ.** Feedback control in active sensing: rat exploratory whisking is modulated by environmental contact. *Proc R Soc Lond B Biol Sci* 274: 1035–1041, 2007.
- Pinto DJ, Brumberg JC, Simons DJ.** Circuit dynamics and coding strategies in rodent somatosensory cortex. *J Neurophysiol* 83: 1158–1166, 2000.
- Pinto DJ, Brumberg JC, Simons DJ, Ermentrout GB.** A quantitative population model of whisker barrels: re-examining the Wilson-Cowan equations. *J Comput Neurosci* 3: 247–264, 1996.
- Sachdev RNS, Berg RW, Champney G, Kleinfeld D, Ebner FF.** Unilateral vibrissa contact: changes in amplitude but not timing of rhythmic whisking. *Somatosens Mot Res* 20: 163–169, 2003.
- Shoykhet M, Doherty D, Simons DJ.** Coding of deflection velocity and amplitude by whisker primary afferent neurons: implications for higher level processing. *Somatosens Mot Res* 17: 171–180, 2000.
- Szwed M, Bagdasarian K, Ahissar E.** Encoding of vibrissal active touch. *Neuron* 40: 621–630, 2003.
- Szwed M, Bagdasarian K, Blumenfeld B, Barak O, Derdikman D, Ahissar E.** Responses of trigeminal ganglion neurons to the radial distance of contact during active vibrissal touch. *J Neurophysiol* 95: 791–802, 2006.
- Temereanca S, Simons DJ.** Local field potentials and the encoding of whisker deflections by population firing synchrony in thalamic barreloids. *J Neurophysiol* 89: 2137–2145, 2003.
- Towal RB, Hartmann MJ.** Right-left asymmetries in the whisking behavior of rats anticipate head movements. *J Neurosci* 26: 8838–8846, 2006.
- Welker WI.** Analysis of sniffing of the albino rat. *Behaviour* 22: 223–244, 1964.
- Wineski LE.** Movements of the cranial vibrissae in the golden hamster (*Mesocricetus auratus*). *J Zool* 200: 261–280, 1983.
- Zucker E, Welker WI.** Coding of somatic sensory input by vibrissae neurons in the rat's trigeminal ganglion. *Brain Res* 12: 138–156, 1969.